Volume 10 Number 4 1981

# Progress in Oceanography

**Editors**

Martin V. Angel

Institute of Oceanographic Sciences, Wormley, Godalming, Surrey

James O'Brien

The Florida State University, Tallahassee, Florida

## Contents



Pergamon Press
Oxford New York Paris Frankfurt

ISBN 0 08 028425 6
ISSN 0079-6611
POCNAS 10(4) 193–226 (1981)

*Prog. Oceanog.* Vol. 10, pp. 193–226.
Pergamon Press Ltd. 1981. Printed in Great Britain

0079-661/81/0801-193 $05.00/0

# Waves and currents near the continental shelf edge

J. M. HUTHNANCE

*Institute of Oceanographic Sciences, Bidston Observatory, Birkenhead, Merseyside L43 7RA.*

(*Received* 24 *April* 1980; *accepted for publication* 24 *January* 1981)

**Abstract**—The abrupt depth increase which characterises the edge of many continental shelves determines a reduced horizontal length scale and a localised transition from shelf seas to the deep ocean. Particular forms of motion which may arise from the steep slopes include topographically guided currents along the slope, shelf-break upwelling, topographic Rossby waves and internal lee waves in the tidal current. The ocean/shelf mismatch may lead to a clear separation of water types, substantial reflection (from the shelf-edge neighbourhood) of all oceanic and shelf motions with periods greater than a few hours, and interaction between barotropic and baroclinic motions. Unstable longshelf currents, interleaving water masses, strong internal tides and internal waves, and narrow canyons enhance mixing across the shelf edge.

## CONTENTS



## 1. INTRODUCTION

THE REGION near the continental shelf edge is of particular interest to oceanographers for the occurrence of motions of both oceanic and shelf origin. Moreover, it is often convenient to model the ocean or shelf separately from each other; shelf-edge boundary conditions correctly representing the transmission, trapping or reflection of various motions are then required. In addition, the reduced topographic length scale and steep slopes are associated with waveforms and motions peculiar to the neighbourhood of the shelf edge.

Various processes lead us to consider a region extending oceanwards at least to the continental slope below the main oceanic stratification. Alternatively, we might characterise

the shelf edge region topographically as an area of steep sea floor slope (relative to typical slopes on the shelf inshore), i.e.

$$h|\nabla h|^{-1} \ll \text{distance to coast}$$

and include a strip of similar width on either side. Such a characterisation is usually appropriate on the coastal side. Baroclinic motions often set an internal Rossby radius of deformation scale

$$R_I = [gh_1h_2(\rho_2-\rho_1)/(h_1 + h_2)\rho_2 f^2]^{1/2} = 0\ (10\,\text{km})$$

for a two-layer model with upper/lower layer densities and depths $\rho_1, h_1/\rho_2, h_2$ respectively; $g$ is gravitational acceleration and $f$ the Coriolis parameter 2 (earth's spin) sin (latitude). When (commonly) $R_I$ or the topographic scale $h|\nabla h|^{-1}$ is much less than shelf width, we have a clear intuitive notion of a narrow shelf edge region seaward of the main shelf area. Ultimately, however, it is important not to impose an arbitrary definition but to let the various physical processes determine their own domains of interest.

Several length scales are indicated by the equations of motion. The momentum and continuity equations for an inviscid non-diffusive stratified sea of depth $h(\mathbf{x})$ may be non-dimensionalised using the following scales: horizontal velocity $U$, time $T$, Coriolis parameter $f$, gravity $g$, reduced gravity $g' \equiv g\Delta\rho/\rho$ (where $\rho$ is a mean density and $\Delta\rho$ a characteristic density difference), depth $H$, characteristic bottom slope $\alpha$ and the earth's radius $R_E$. Since the ocean is relatively shallow, the earth's radius has little geometric significance, and $R_E$ is conveniently represented by $\beta\ (\sim R_E^{-1})$, the northward gradient of $f$. The pressure and vertical velocity scales are then determined by the momentum and continuity equations respectively. Seven independent length scales result; non-dimensional combinations make the choice somewhat arbitrary and the following is merely conventional: particle excursion $UT$, $U/f_0$, depth $H$, gravity 'wavelength' $(gH)^{1/2}T$, Rossby 'wavelength' $R_B \equiv (\beta T)^{-1}$, internal Rossby deformation radius $R_I \equiv (g'H)^{1/2}f_0$ and the topographic scale $H/\alpha$. The length scale $L$ in any particular context is normally the minimum of the last four, except that $R_I$ does not influence barotropic motion.

Six non-dimensional ratios result. The Rossby number $\varepsilon \equiv U/f_0L$, or UT/L for motions above the inertial frequency, measures the intensity ($U$) and non-linearity of the motion. Typical oceanic scales imply $\varepsilon \ll 1$, i.e. linearity. However, the small shelf-edge topographic scale tends to increase $\varepsilon$, encouraging non-linear effects. Energy may be transferred to different frequencies or to mean currents, and to wave motions from unstable mean currents, although the sea floor slope itself is generally stabilising. The aspect ratio $\delta \equiv H/L$ is usually small except for (i) internal motions at frequencies (several cycles per hour) comparable with $N \equiv (-g/\rho\, d\rho/dz)^{1/2}$, the Brunt-Väisälä or buoyancy frequency; (ii) high frequency surface waves with periods of less than a minute or so in a depth of 200 m (say). However, the latter decay downwards and are less influenced by the sea floor; only surface waves with periods greater than one minute experience amplitude increases exceeding 10% on entering 200 m depth from the deep sea, i.e. only small-$\delta$ 'long' surface waves 'see' the shelf edge directly. Small $\delta$ is associated with approximately hydrostatic pressure. The internal Froude number $F \equiv U^2/(g'H)$ relates the flow speed $U$ to the long internal gravity wave speed $= 0(g'H)^{1/2}$, e.g. $[gh_1h_2(\rho_2-\rho_1)/(h_1 + h_2)\rho_2]^{1/2}$ in a two-layer model. Sufficiently rapid flows ($F > 1$) are supercritical in the hydraulic sense, e.g. $U > 0.2$ m/sec if there is a 25 m surface layer with a density reduction of 0.2 $\sigma_T$ units, conditions typical of tidal currents and the initial spring stratification on the North west European shelf (CARTWRIGHT 1976; ELLETT and MARTIN 1973). The divergence parameter $D^2 \equiv L^2/(T^2gH)$ is small when the length scale $L$ is much

less than the gravity wavelength $(gH)^{1/2}T$. Surface displacements then play a negligible role in the mass balance, leading to the common approximation of negligible horizontal divergence for motions of sufficiently long period $2\pi T$. At the other extreme, ray theory (e.g. SHEN, MEYER and KELLER, 1968) may be applied to gravity waves when $H/\alpha \gg (gH)^{1/2}T$, i.e. ambient conditions change little for the gravity wave in one wavelength. The intermediate case of strong interaction, $(gH)^{1/2}T \sim H/\alpha \sim 10\,\text{km}$ (say), occurs for gravity wave periods $2\pi T$ of several minutes (23.4 min if $H = 200\,\text{m}$). The motion is then horizontally divergent but the gravity wave form is strongly affected by the sloping bottom. Finally, two ratios may be formed from the internal deformation radius $R_I$ (typically 0(10 km) on the shelf), the topographic scale $H/\alpha$ (typically 0(10 km) near the shelf edge), and the Rossby 'wavelength' $R_B$. $R_B \lesssim 10\,\text{km}$ for barotropic Rossby waves of period $\gtrsim 1$ year. However, Rossby waves depend on potential vorticity gradients, to which the depth gradient contributes overwhelmingly near the shelf edge. Hence $R_B$ is best compared with $R_I$ away from the shelf edge and large depth gradients. Then baroclinic Rossby waves are only possible at sufficiently low frequencies: $R_B \lesssim R_I$. Higher frequency Rossby waves must be barotropic; these longer waves then tend to see the shelf edge region as a scarp, where they are almost totally reflected (Section 5 below). The comparability of $R_I$ and $H/\alpha$ implies matching of the bottom slope with the characteristic slope of internal waves near the inertial or tidal frequencies. Strong internal tide generation may result (Section 9 below), and topographically trapped waves below the inertial frequency may be significantly modified by the stratification.

Diffusion is essential to the description of steady state upwelling. Indeed, spatially varying eddy viscosity is the agent of one shelf-edge upwelling mechanism described at the end of Section 4. Apart from this and double-diffusive effects, however, diffusion tends to control the final form rather than the initial possibility of the various phenomena. Accordingly, we do not explicitly treat diffusive length scales, which are usually less than $L$ and, subject to the above, play a passive role. In particular, the onset rather than the steady state of 'conventional' upwelling is considered. This has the advantages of simplicity and a clearer separation of cause and effect.

Longshelf variations in the shelf topography or the flow may define a separate length scale $\Lambda$, generally greater than the cross-shelf scale $L$ near the shelf edge. Its dynamical significance for the flow depends on the time scale $T$; increased geostrophic guidance at long periods $T \gg f_0^{-1}$ gives longshelf variations an enhanced role, roughly as $f_0 TL/\Lambda$. Near and below the inertial period, significant local effects generally require $\Lambda/L = 0(1)$. However, shelf variations of length scale $\Lambda$ strongly affect waves of length $\Lambda$ or more, no matter how large $\Lambda/L$ may be.

The two time scales $T$ and $f_0^{-1}$ combine as $Tf_0$ indicating the period of the motion relative to an inertial period. The following sections are roughly in order of decreasing $Tf_0$ although the separate treatment of individual phenomena takes priority. As hinted above, a lower limit $2\pi T \sim 1$ minute is set where the shelf-edge topography ceases to have any substantial effect on the motion.

## 2. WATER MASSES

The small depths and consequent reduced thermal capacity of continental shelf seas are liable to increase the temperature effects of summer heating and winter cooling in comparison with the adjacent ocean. (A famous example of the latter is the localisation of Antarctic Bottom Water formation to the Weddell Sea, where winter cooling and ice formation over the shelf play a key role: SVERDRUP, JOHNSON and FLEMING 1946, pp.

609–612). The input of fresh river-water at the coast may help to form shelf water distinct from that of the adjacent deep sea. Moreover, stirring from below by the stronger tidal current sharpens the seasonal thermocline in the Middle Atlantic Bight (say) relative to that in deeper water, isolating relatively cold water on the shelf below the summer thermocline (MOOERS, GARVINE and MARTIN, 1979). Further inshore, the tidal currents $U$ increase sufficiently to stir throughout the reduced depth $H$ according to the $U^3/H$ criterion of SIMPSON and HUNTER (1974). Surface fronts of the type common on the North-west European shelf (e.g. PINGREE, 1979) may then form between cooler well-mixed water inshore and the warmer summer surface layer offshore. The front will occur at the edge of a shelf shallow or broad enough to be tidally well-mixed.

For these various reasons, abrupt changes of water type near the shelf edge occur widely, as shown by satellite pictures (e.g. LEGECKIS, 1978). The Middle Atlantic Bight is a well-documented example (Fig. 1). WRIGHT (1976) used a shelf-water criterion $T < 10°C$ (or $S < 35°/_{oo}$ for summer-heated surface water) to find that the shelf-water boundary at the bottom remained within 16 km ($\pm 20$ m in water depth) of the 100 m depth contour 84 % of the time. The position of the boundary on the sea-surface is more variable but may be quite coherent and sharp; VOORHIS, WEBB and MILLARD (1976) show a striking satellite photograph from late winter when the shelf water is coldest. The Bering Sea also shows a large (but broader) salinity increase across the shelf edge. This gives a salinity flux from the deep sea onto the shelf, balancing the large fresh water runoff into the well-mixed shelf water (KINDER and COACHMAN, 1978).

Any fresh-water contribution to the shelf water tends to make it less dense than the adjacent ocean, at least in summer (all the year off New England). The boundary between water masses then slopes off-shore from the bottom to the surface, and there is an associated offshore drop in sea surface level and a near-surface geostrophic flow, cyclonic about the deep sea, even with friction present (CSANADY, 1979). FLAGG and BEARDSLEY (1978) find that the geostrophic guidance of the depth contours may render the New England shelf-edge flow stable in the presence of dissipation, in contrast with strong instability if it were over the interior shelf. They suggest that this may cause the shelf-edge location of the front.

The offshore frontal slope tends towards the horizontal if the wind opposes the associated geostropic flow (CSANADY, 1978a), particularly for small density contrasts across the front.

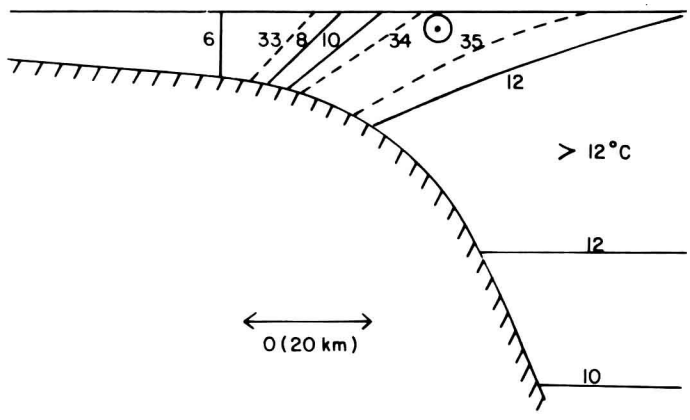


FIG. 1. Sketch of Middle Atlantic Bight shelf-edge conditions in late winter (after Wright, 1976; Voorhis et al., 1976). Salinity in $°/_{oo}$ (– – –), temperature in °C (———). Surface along-shelf current ⊙.

Hence a substantial overall shelf-slope density difference is probably required to establish a front rising to the surface.

Infra-red satellite pictures of surface temperatures off Washington and British Columbia in the North-east Pacific show considerable spatial variability but no indication of the shelf edge position (MYSAK, 1977; TABATA and KIMBER, 1979). Further north in the Gulf of Alaska there is no sharp front, but the shelf water is warmer than over the adjacent slope in summer, and, remarkably, in winter, when mixing distributes cooling through the total depth on the shelf as opposed to a thinner surface layer above the (salinity) stratification off the shelf (ROYER and MUENCH, 1977). The North-west European shelf edge has no rapid transition from shelf to slope water at any season, and the position of the shelf edge could not usually be estimated from temperature and salinity measurements in the overlying water, e.g. I.C.E.S. (1962), ELLETT and MARTIN (1973). (However, cooler surface water near the Celtic Sea shelf edge has often been observed in satellite photographs (PINGREE, 1979): see Section 11). During the summer, thermal stratification above the shelf edge depth extends well onto the shelf and shows topographic influence only in a sharpening of the lower side of the thermocline by the stronger tidal currents on the shelf (Fig. 2). The underlying water over the shelf edge only warms significantly from its late winter temperature when autumnal mixing through the total shelf depth occurs. This suggests that late winter conditions largely control the absence of any shelf-edge fronts. Then the temperature and salinity increase smoothly from coastal to deep-sea values across the whole width of the shelf. By contrast with the New England context, milder winters, less influence from fresh water (which tends to be geostrophically guided through the eastern North Sea to the Norwegian coast), greater mixing by tidal currents and winter storms, and in some places an extremely irregular shelf edge probably all play a part in avoiding any abrupt changes near the North-west European shelf edge.

Mixing across the shelf edge occurs in many ways, which are discussed further in Section 11. However, large shelf-edge gradients tend to imply a *reduced* total diffusivity there compared with adjacent shelf and deep-sea regions. As suggested in the New England context, geostrophic guidance along the shelf edge and adjacent steep slope inhibits exchange between the water masses to either side, which thus acquire local characteristics, particularly over the shelf.

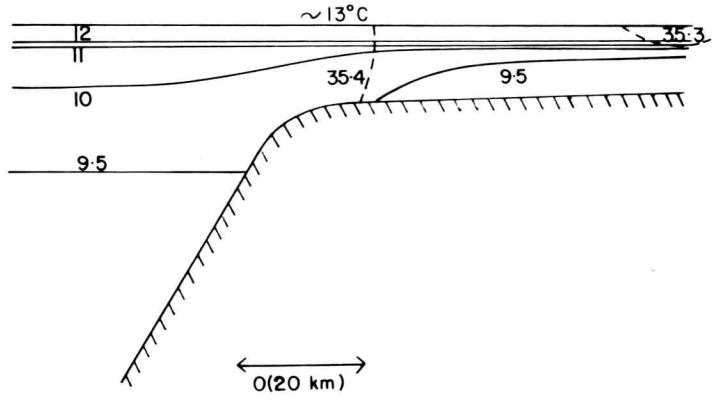


FIG. 2. Sketch of the North-west European shelf edge in June (after Ellett and Martin, 1973). Salinity in ‰ (——), temperature in °C (———).

Strong geostrophic flows are encouraged by the juxtaposition of different water types, and also by the convergence of depth contours where the shelf break is sharp. Furthermore, the major western boundary currents often follow a scarp for a large part of their well-defined course. Examples are the Florida current/Gulf Stream north to Cape Hatteras, and the Agulhas current off South Africa, particularly where the continental slope is steep (PEARCE, 1977). These currents advect another water type distinct from that on the shelf. Where such strong currents lose the shelf-edge guidance, they appear to be major sources of eddies (WYRTKI, MAGAARD and HAGER, 1976). However, the Gulf Stream rings associated with shelf-water release in the Middle Atlantic Bight (e.g. MORGAN and BISHOP, 1977) themselves remain seaward of the shelf edge, reducing their potential for inducing shelf/slope exchange. While still guided by the shelf edge, a strong current may be unstable, meandering and spinning off small eddies. However, the effects of these are also observed to diminish rapidly inshore of the shelf edge (PEARCE, 1977; LEE and BROOKS, 1979), perhaps on the internal deformation scale $R_I$ (see Section 5).

## 3. LONG-PERIOD WAVES

The steep slopes near the shelf edge imply a large potential vorticity gradient. A fluid column displaced up or down the slope, and conserving potential vorticity, acquires relative vorticity. This is manifested as displacements by adjacent columns; the result is long-shelf propagation of the disturbance in a cyclonic sense about the deeper water. Such wave motions are known as continental shelf waves (ROBINSON, 1964) and, over a mid-ocean scarp, as double-Kelvin waves (RHINES, 1967; LONGUET-HIGGINS, 1968). It is known (HUTHNANCE, 1975) that for a straight shelf with any monotonic depth profile there is an infinite set of wave modes, with 1,2... offshore nodes. Each mode $n$ has a dispersion relation $\sigma = \sigma_n(k)$ for the frequency as a function of longshore wavenumber $k$, which for small $k$ gives a constant phase speed $\mathrm{d}\sigma_n/\mathrm{d}k$. The frequencies $\sigma_n$ decrease with n from $\sigma_1 < f$. In unstratified conditions the (barotropic) current magnitude varies spatially roughly as $h^{-1/2}$; the modal structure is distributed roughly as $(h^{-1}\,\mathrm{d}h/\mathrm{d}x)^{1/2}$ and is therefore concentrated near any well defined shelf edge (Fig. 3). Shelf waves and double Kelvin waves are thus seen to be manifestations of the same phenomenon, differing only in whether the coast is far enough from the shelf edge for the motion at the latter to be regarded separately (the double Kelvin wave).

All the above qualitative conclusions extend to stratified conditions (HUTHNANCE, 1978a), particularly since the stratification is effectively weak ($R_I \ll$ shelf width) on most shelves broad enough to have a well-defined edge. A few of the modes may take the form of internal Kelvin waves at the coast if $R_I > H/\alpha$ there. However, the majority of the modes cluster near the shelf edge; here there is a reduced topographic scale $H/\alpha$ and quite possibly $R_I \gtrsim H/\alpha$, so that the wave modes include an element of gravity wave dynamics (for $R_I \gg H/\alpha$ they adopt internal Kelvin-like wave forms against the steep slope). For short long-shelf wavelengths, they take the form of bottom-trapped waves (RHINES, 1970) of frequency $\sigma \simeq N\alpha$ and located near the sea-floor maximum of $N\alpha$ ($N^2 \equiv -g/\rho\,\mathrm{d}\rho/\mathrm{d}z$). This maximum is usually near the shelf edge. Its representation is a severe test of any model.

Continental shelf waves are most readily generated by wind stress along the shelf (ADAMS and BUCHWALD, 1969), and so typically have periods of several days. A simple picture of the way a long shelf wave is built up by local forcing as it progresses has been developed by GILL and SCHUMANN (1974). Waves forced meteorologically have been observed along the coast of Australia (HAMON, 1966), North Carolina (MYSAK and HAMON, 1969), Oregon (CUTCHIN and SMITH, 1973), Western France (LIE, 1979) and elsewhere, albeit often only in coastal sea level.

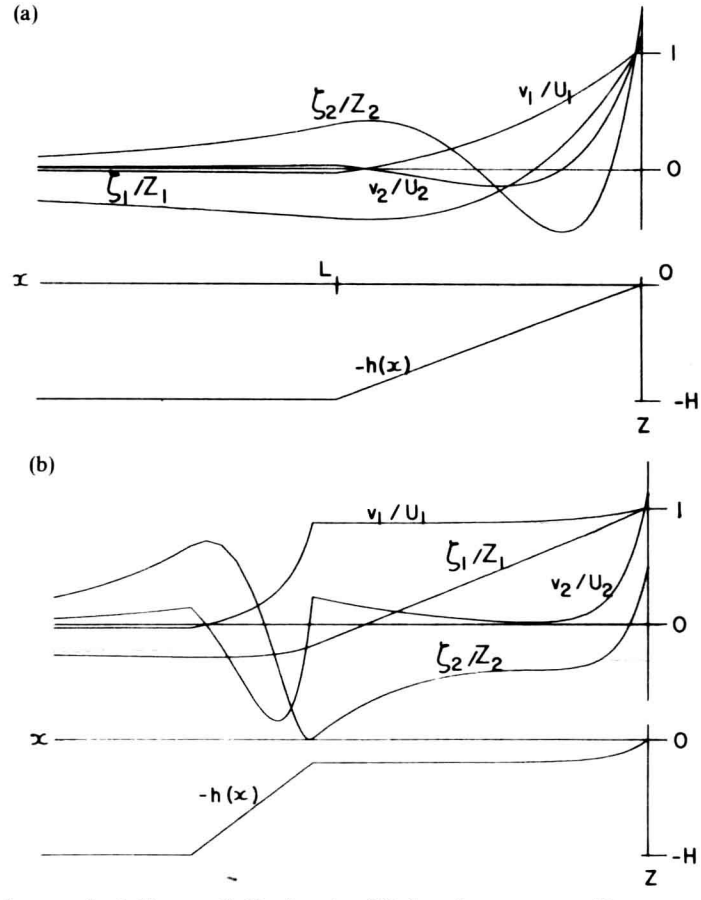


FIG. 3. First two barotropic shelf waves (1, 2): elevation $\zeta/Z$, longshore current $v/U$.
(a) $h = Hx/L$ $(0 < x < L)$, $h = H(x > L)$, $k_1L = 0.415$, $Z_1/U_1 = 0.232fL/g$
$k_2L = 1.446$, $Z_2/U_2 = 0.0592fL/g$

(b) $h = 0.2\ H(1 - \exp(-10 - 5x/L))(-2L < x < 0.2L)$,
$h = Hx/L(0.2L < x < L)$, $h = H\ (x > L)$, $k_1L = 0.0609$,
$Z_1/U_1 = 1.64fL/g$, $k_2L = 1.196$, $Z_2/U_2 = 0.197fL/g$. In both cases $f^2L^2/gH = 0.0025$, $\sigma/f = 0.1$

Current meter measurements support the interpretation off Oregon and also show shelf waves dominating the longshore current in the Peruvian upwelling region (BRINK, HALPERN and SMITH, 1980). Wind induced currents of 0(10–20 cm/sec) appear to be typical. Most observations have been of the (fastest) first mode, consisting primarily of a longshelf current which is typically fairly uniform across the shelf (Fig. 3) and confined to the shelf. This mode appears to be the natural and direct response to a wind stress along the shelf (in the same sense that surface waves are a natural response to atmospheric pressure fluctuations). Accompanying sea level changes are greatest at the coast and relatively small near the shelf edge (Fig. 3), as observed in the Middle Atlantic Bight (BEARDSLEY, MOFJELD, WIMBUSH, FLAGG and VERMERSCH, 1977).

Shelf-wave forms also play an important role in low frequency oceanic-scale motions, by which they are forced in order to satisfy in detail the boundary condition of no flow through the oceanic 'sidewall' i.e. the continental slope and shelf (ALLEN, 1976; HUTHNANCE, 1978b).

SMITH and LOUIS (1979) have observed waves in the Nova Scotia surface front (0(100 km) seaward from the shelf break) induced by warm core Gulf Stream eddies further offshore and to the west. Shelf waves contribute to the K1 diurnal tide on the North-west Scottish shelf, where they reduce coastal elevations to half the adjacent shelf-edge values (CARTWRIGHT, HUTHNANCE, SPENCER and VASSIE, 1980); they are probably generated by interaction of the oceanic K1 wave with the irregular shelf west of the British Isles.

Observations of internal Kelvin waves and shelf waves in stratified contexts have been reviewed by CLARKE (1977). Bottom trapped waves have probably been observed near site *D*, where $N\alpha \simeq 1/8$ cycle per day (THOMPSON and LUYTEN, 1976). They can also exist above the inertial frequency and, for example, perhaps play a part in the large quarter-diurnal tidal currents noticed by GORDON (1979) off North west Africa. These occurred near the bottom in 400 m of water where $N\alpha$ was near 4 cycles per day, a large value (but not unusual, see section 9) resulting from the conjunction of substantial stratification with the steepest portion of the shelf profile.

A longshore current, unlike stratification, may affect the waves' qualitative modal distribution (NIILER and MYSAK, 1971); it advects the waves and slower modes may even be reversed to propagate anticyclonically about the deep sea. Moreover, its shear modifies the background potential vorticity; if the gradient of the latter is anywhere reversed a new set of modes may exist, also propagating in the reverse sense. Potential vorticity extrema roughly corresponding to shear maxima, and short-scale spatial irregularities across the longshore current (HELBIG, 1980), may also lead to instability of the modes at some longshore wavenumbers. This is the counterpart to the instability of plane shear flow, and the depth gradient has a generally stabilising effect. However, examples do exist of shear flows which are stable over uniform depth but unstable over some depth profiles (COLLINGS and GRIMSHAW, 1980; PEDLOSKY, 1980). A mean current which varies in depth and is therefore associated with sloping isopycnals may also be baroclinically unstable. Resulting meanders in the Gulf Stream and Agulhas current have already been mentioned in Section 2. Examples from eastern ocean boundaries are wave forms in sea-surface temperature and salinity off British Columbia, apparently deriving from the California undercurrent (MYSAK, 1977), and fluctuations in the Norwegian Current of a period of 2–3 days (MYSAK and SCHOTT, 1977). (SCHOTT and BOCK (1980) confirm the baroclinic instability and wavelength of the Norwegian Current fluctuations, but calculate a more rapid barotropic energy transfer *from* the fluctuations to the Current, so that the fluctuation-energy budget is unresolved).

Current knowledge of the scope for wave–wave interaction and instability of larger amplitude shelf waves has been considered by MYSAK (1980). These include the interesting possibility of resonant subharmonic response to a travelling wind field (BARTON, 1977).

MYSAK (1980) also reviews the effects on shelf waves of topographic irregularities and longshelf variations. If the latter have a spatial scale $\Lambda$ longer than the wavelength, the shelf wave evolves as it progresses to adopt the local mode form while maintaining its frequency, mode number and longshelf energy flux. ALLEN and ROMEA (1980) find a similar result in stratified conditions for the lowest mode propagating away from the equator, despite its change of form (as $f$ increases so that $R_I$ decreases) from an internal Kelvin wave ($R_I >$ shelf width) to a shelf wave ($R_I <$ shelf width). Short-scale irregularities scatter energy into other modes; see also WANG (1980). At the sides of canyons in the shelf edge (for example), upwelling may occur.

Indeed, upwelling (see the following section) is an important phenomenon associated with shelf waves; it may also be propagated along the shelf by them. Other physical roles of the

waves derive from their ability to transfer momentum (GARRETT, 1979) and heat, salt and nutrients onto the shelf (SMITH, 1978).

All these long waves are manifested as currents (predominantly along the shelf for frequencies much below the inertial frequency) and as internal elevations of magnitude 0 [min $(UH/Lf_0,\ U/N)$] rather than as surface displacements, which are of magnitude $0(f_0UL/g)$, $L$ being the local topographic scale $H/\alpha$. For $L \sim 10$ km near the shelf edge this is only 1 cm for a 10 cm/sec current, but coastal values may be greater with $L$ representing the shelf width. The whole topic of shelf waves has recently been reviewed by MYSAK (1980).

## 4. UPWELLING

The 'classical' upwelling scenario is a coast on the east side of an ocean with an equatorward wind stress $\tau$. Coastal upwelling is required to supply the offshore Ekman transport (e.g. DEFANT, 1961). A simple two-layer model with wind stress acting on the whole upper-layer depth (YOSHIDA, 1955; see DEFANT) nicely illustrates the development of this condition, including an equatorward coastal jet in the upper layer. The phenomenon may occur for all coastal orientations provided only that there is a longshore wind-stress component in the above sense; downwelling occurs if this is reversed.

A similar two-layer model (Fig. 4: in fact considered earlier by DEFANT (1952) with an oscillatory onshore wind) demonstrates the onset of upwelling over a sea-floor scarp parallel to the coast. If this model shelf is wide ($\gg R_I$) and the ocean depth is large, such shelf-edge upwelling is a fraction $h_1/[h_2 + (h_2H)^{1/2}]$ of the coastal rate $\tau(g\rho\Delta\rho h_1H/h_2)^{-1/2}$ according to the model. Under favourable conditions the interface may thus rise some metres per day. The

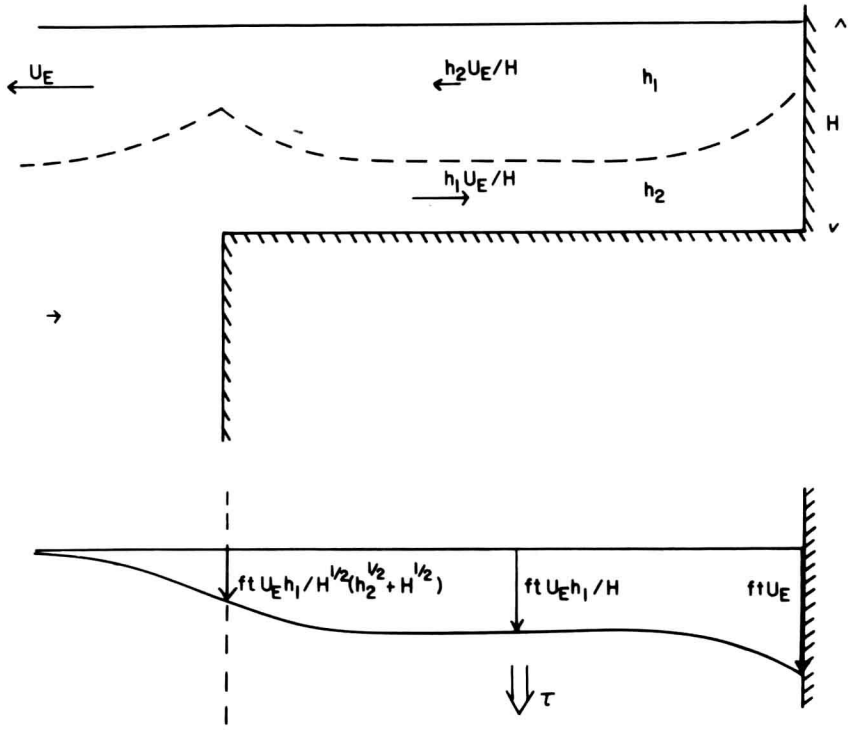


FIG. 4. Two-layer upwelling. (a) section, (b) Northern hemisphere upper layer plan. $U_E \equiv \tau/\rho f h_1$.

upwelling decays to either side of the scarp over the respective internal deformation radii $R_I$. Likewise the offshore and longshore currents tend to their uniform-depth values on the same scale. The shelf-edge upwelling arises because (i) the total shoreward flux summed over both layers is zero and (ii) *relative* to the lower layer flow, the upper layer offshore flux is (wind stress)/$f$ far ($\gg R_I$) from boundaries. In the deep lower layer off the shelf, the compensating inshore flow is slow by (i). Hence (ii) implies that the offshore flow in the upper layer is faster off the shelf than on the shelf. The shelf-edge upwelling feeds this upper layer divergence. Evidently shelf-edge and coastal upwelling are only distinct if the shelf width is sufficient ($\gtrsim 2R_I$).

CSANADY (1973) used a similar model with a sloping shelf to find the response to longshore and onshore winds. JOHNSON (1981) also considers a time-dependent model to find shelf-break upwelling proportional to (change of bottom slope)/(shelf depth). JANOWITZ and PZETRAFESA (1980) found shelf-break upwelling if (similarly) the bottom slope changes rapidly there.

Steady-state calculations by LILL (1979) confirm the existence of upwelling in a homogeneous sea just offshore from a smooth shelf break. Steady-state upwelling in various shelf-edge contexts has also been considered theoretically by TOMCZAK and KÄSE (1974). JOHNSON and KILLWORTH (1975) and HSUEH and OU (1975). JOHNSON and MANJA (1979) considered a level shelf meeting a slope. Over the slope, horizontal diffusion increases the onshore transport in the bottom boundary layer beneath a steady longshore flow. This tends to give bottom boundary layer convergence at the shelf break. However, they found that in the (final) steady state the consequent shelf-break upwelling cannot be accommodated by the water above. Instead, there is shear in the longshore current over the shelf break.

The above models are all 'local'. GILL and CLARK (1974) emphasised that coastal upwelling may also be caused by propagating long waves (Section 3) generated elsewhere on the shelf. This applies equally to shelf-edge upwelling. Narrow-shelf examples are off Peru, where shelf waves with longshore gradients upset the local mass balance in the vertical offshore plane (BRINK *et al.*, 1980) and in the Gulf of Guinea, where CLARKE (1979) has interpreted upwelling in terms of westward-propagating waves generated by winds several hundred kilometres further east. The upwelling may also depend on a prior raising of thermocline level in summer as the Guinea current intensifies due to winds over the whole equatorial Atlantic (PHILANDER, 1979).

BANG and ANDREWS (1974) observed a strong upwelling — associated current just seaward of the South-west Africa shelf break, which they believed to be amplified by a wind profile intensifying inshore. Off North-west Africa the coastal upwelling is observed to migrate to the shelf edge in a few days if the favourable winds persist (BARTON, HUYER and SMITH, 1977). In the southern Middle Atlantic Bight, BOICOURT and HACKER (1976) found that the offshore surface Ekman flux driven by a southerly wind was replaced beneath by saltier slope water drawn onto the shelf.

A poleward undercurrent is frequently found in association with upwelling. Off northwest Africa this flows below the shelf break (MITTELSTAEDT, PILLSBURY and SMITH, 1975), whereas off Oregon the shelf break is less sharp and the undercurrent is partly on the shelf (HUYER, 1976). A steady-state diffusive model (MCCREARY, 1981), with only a flat bottom and coastal wall, simulates this undercurrent and its poleward extension beyond the region of upwelling-favourable winds.

Some continental shelves, notably the Celtic Sea and off Southern California, are indented by numerous canyons. SHAFFER (1976) has seen some evidence of shelf-edge canyons guiding upwelling off North-west Africa. PEFFLEY and O'BRIEN (1976) have found numerically that

enhanced upwelling occurs on the equatorward side of a canyon near the coast. Moreover, KILLWORTH (1978) has found analytically that a propagating internal upward displacement (upwelling) (i.e. an internal Kelvin wave of finite extent) leaves residual steady upwelling on the equatorward side of a canyon. These results almost certainly apply also to canyons at the shelf edge. GILL and SCHUMANN (1979) considered a two-layer model with a strong upper layer current (Froude number 0(1)) of speed comparable with that of long internal waves, along a shelf and scarp of varying width. They found that upwelling (surfacing of the lower layer in a coastal strip) may occur at a western ocean boundary, downstream of a narrower shelf section in a poleward current. This appears to be manifested by the Agulhas current south of 32°S off South Africa.

Shelf-edge upwelling may have (at least) two other causes. HEAPS (1980b) has suggested a mechanism appropriate to the Celtic Sea shelf edge in summer, when the thermocline over the shelf is sharper than off the shelf. This 'slippery' interface beneath the heated upper layer over the shelf facilitates circulation *within* that layer in a vertical offshore plane. Winds driving coastal *downwelling* then induce upwelling within the upper layer near the shelf edge where the interface ceases to be 'slippery'. WUNSCH (1970) pointed out that the stable oceanic temperature stratification, combined with a condition of zero heat flux through the sea floor at the continental slope, implies a dip of the isotherms there, and a tendency for upwelling in a thin layer against the slope; however, this may be complicated if the salinity stratification is unstable. WUNSCH shows temperature profiles with decreasing gradients towards the sides of Bermuda (ie. the lower contours dip towards the slope) and rough steps indicative of stirring.

The shelf-edge upwelling observations cited above are considerably outnumbered by the models. However, in many upwelling contexts the shelf width is less than $2R_I$ (particularly in the tropics) and coastal and shelf-edge upwelling merge. The shelf-edge contribution is no less real for not being separately apparent, and the variety of models acknowledges the important role of shelf/slope topography in upwelling.

## 5. EDDIES

A large proportion of the oceanic kinetic energy at frequencies much less than the inertial frequency is found to be in fluctuations with periods of months and length scales of order 100 km (the MODE group, 1978). Such 'mesoscale eddies' are thought to be governed by Rossby wave dynamics, i.e. they propagate by the same means as shelf waves (Section 3), but the background potential vorticity gradient derives from the latitudinal variation of the inertial frequency $f$. Their length scale $R_B$ and period $2\pi T$ are related by $R_B = (\beta T)^{-1}$ (Section 1); for sufficiently long periods (typically $\gtrsim 1$ year) so that $R_B \lesssim R_I$, baroclinic as well as barotropic forms are possible. (A sloping sea floor permits baroclinic Rossby waves at higher frequencies ($R_B > R_I$) but also causes interaction between barotropic and baroclinic forms). It is clearly desirable to assess the behaviour of such important oceanic motions on encountering the continental shelf.

There appears to be a tendency for eddies to stop short of the shelf edge. The many observations discussed by LAI and RICHARDSON, (1977) and RICHARDSON, CHENEY and WORTHINGTON (1978) seem to show this. Even Gulf Stream rings associated with tongues of surface shelf-water extending off-shelf from the Middle Atlantic Bight (MORGAN and BISHOP, 1977; HALLIWELL and MOOERS, 1979) apparently remain off the shelf. MOOERS *et al.* (1979) similarly found an off-shelf extension of cold ($<8$°C) bottom water between eddies, but otherwise this cold water just inshore of the shelf break was little disturbed: the eddies penetrated to the shelf break but not much further.

Gulf stream meanders and eddies appear to reach further onto the shelf to the south, where the Stream runs along the slope close (in terms of $R_I$) to the shelf break. LEE and MAYER (1977) and VUKOVICH, CRISSMAN, BUSHNELL and KING (1979), say, report meanders and eddies (elongated along-shelf) on the narrow Florida shelf. On wider shelves, there appears to be a decrease, inshore from the shelf edge, of the effects of meanders and eddies spun off from (for example) the Gulf Stream on the Georgia shelf (LEE and BROOKS, 1979) and the Agulhas current off South Africa (PEARCE, 1977). On the shelf, further than perhaps $0(R_I)$ from the shelf break, the currents tend rather to be driven by local winds.

KROLL and NIILER (1976) considered theoretically the transmission of barotropic Rossby waves (allowing for an exponentially sloping sea floor) across changes of bottom slope $\alpha$; any significant change leads to substantial reflection unless two parallel such changes are appropriately spaced. A *two-layer* model with a straight vertical scarp between regions of uniform depth indicates almost total reflection in $R_E \gg R_B > R_I$, i.e. at frequencies much less than the inertial frequency (HUTHNANCE, 1981). This agrees with the barotropic calculation (LE BLOND and MYSAK 1978, p. 204), as expected from the resistance to ageostrophic displacements over the step. At still lower frequencies such that baroclinic Rossby waves are possible, there may be substantial scattering into a transmitted barotropic wave and transmitted and reflected baroclinic Rossby waves, provided the stratification extends over the shallower side (shelf).

The tendency to transmit only low frequencies implies shorter length scales ($R_I$) over the shelf. However, KROLL and NIILER (1976) point out that these low frequency motions will there be subject to relatively rapid dissipation. Hence even with "transmission" the influence of oceanic eddies may penetrate only $0(R_I)$ onto the shelf past a sharp shelf edge. This contrasts with the greater penetration onto the shelf achieved by oceanic-scale motions forcing shelf wave forms (Section 3).

The nature, and extent onto the shelf, of eddies spun off a current along the slope probably represents the fastest-growing long-wave instability of the current, a topic touched on in Section 3 (see also MYSAK, 1980). A variety of shelf geometries (especially widths) and current profiles need to be considered to develop an understanding.

Reflection or effective absorption of Rossby waves approaching the shelf implies a transfer of their momentum flux, which appears as a forcing function for the 'mean' pressure and flow fields. GARRETT (1979) has suggested that topographic Rossby waves at least partially balance the pressure gradient along the East Australian coast, and are effective in transferring this offshore to drive the East Australia current. One may speculate that the paths of SOFAR floats 2 and 14 during MODE (RISER, FREELAND and ROSSBY, 1978) might indicate a similar process; they were caught in vigorous eddying motions until encountering a strong southward current near 76°W, 30°N over the foot of the continental slope. CSANADY (1978b) infers an oceanic origin for the overall pressure gradient along the New England shelf, and CHASE (1979) found Gulf Stream position to be the predominant factor in absolute coastal pressure in the Middle Atlantic Bight.

To summarise, it seems unlikely that eddy motions will extend further than $0(R_I)$ onto the shelf. However, even eddies not reaching the shelf at all may induce waves in a shelf water/slope water front sloping oceanwards from the shelf break (SMITH and LOUIS, 1979) and likewise entrain surface shelf water (see Section 11). Moreover, they are another potential source of quasi-geostrophic fluctuating and mean currents guided along the shelf edge. Any associated longshelf gradient of mean pressure (surface elevation) may extend across the shelf to influence the on-shelf circulation.

## 6. INERTIAL MOTIONS

At frequencies close to the local inertial frequency $f$, the field equation for internal motion in inviscid, stratified fluid reduces to a constraint on the horizontal structure. For a harmonic constituent $\exp i(ft + ky)$ freely propagating along a uniform shelf of arbitrary depth profile $h(x)$, offshore decay as $\exp(-kx)$ is required. Since $k > 0$, this implies cyclonic propagation about the deep sea. The interior dynamics do not constrain the vertical structure, which is determined by the (effectively lateral) sea floor boundary condition $w = -u\,dh/dx$; the perturbation pressure satisfies a second-order ordinary differential equation in $z$ (HUTHNANCE, 1978a). The barotropic Kelvin wave (see next section) is always a solution, so that the coastal boundary enables energy propagation at the inertial frequency. Baroclinic motion is possible if $N dh/dx > f$ somewhere on the sloping bottom.

Figure 5 illustrates the simplest baroclinic form near a shelf edge where a gently sloping shelf meets a steeper continental slope. By conservation of mass, the vertical velocity $w$ is continuous in $z$. Hence the sharp shoreward decrease of $|dh/dx|$ at the top of the slope implies (through the boundary condition) a sharp increase of the on–offshore velocity $u$.

Near the shelf edge (near the shelf edge *depth* particularly) we can expect greater vertical velocities than typical shelf values and greater horizontal velocities than typical slope values, with strong shear between depths. Owing to the sloping sea floor, the horizontal velocity components are *not* circularly polarised; Fig. 5 shows anticyclonic polarisation near the surface and cyclonic polarisation towards the bottom of the slope. Associated internal elevations are $0(U\alpha/f)$, and surface displacements are $0(fUL/g)$.

In an unbounded fluid with a non-zero vertical coefficient of kinematic viscosity $\nu$, changes in the surface wind stress give rise to inertial currents, which propagate downwards with speed $(2\nu f)^{1/2}$ and penetration depth $(2\nu/f)^{1/2}$. However, lateral boundaries imply in addition a change of surface slope when the wind stress changes. KRAUSS (1979) demonstrates that this results in a second set of inertial waves, which occur at all depths within a fraction of an inertial period because the pressure gradient beneath the surface slope acts throughout the depth. In the shelf-edge context this suggests that inertial motions which penetrate down to

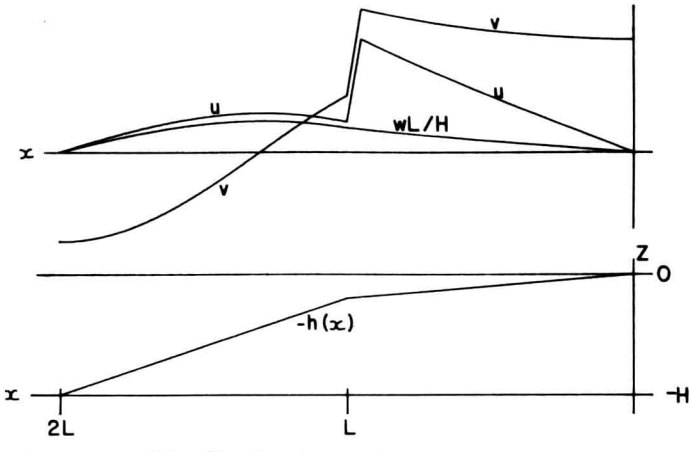


FIG. 5. First trapped wave at $\sigma = f$. Profiles of onshore ($u$), longshore ($v$) and vertical ($w$) velocity components on the sea floor $z = -h(x)$ where $h = 0.2Hx/L$ $(0 < x < L)$, $h = -0.6H + 0.8Hx/L$ $(L < x < 2L)$, $h = H$ $(x > 2L)$. $u, v, w \propto \exp(-kx)$ where $kL = 0.97$, $f^2L^2/gH \ll 1$, $N^2H^2/f^2L^2 = 10$.

the shelf-edge depth may then propagate rapidly to much greater depths down the slope, albeit with much reduced amplitude owing to energy constraints. Where the sea floor slope $\alpha$ *is critical:* $\alpha = (\sigma^2 - f^2)^{1/2}/(N^2 - \sigma^2)^{1/2}$, the currents may be amplified several times within an $0((Hfv/2N^2\alpha^2)^{1/3} \sim 20\,\mathrm{m})$ bottom boundary layer (GORDON, 1980). As $\alpha \downarrow 0$ with $\sigma \downarrow f$, this layer may be thick, as remarked by Weatherly, Blumsack and Bird (1980) for the flat-bottomed case when the thickness is $0(\nu/(\sigma - f))^{1/2}$.

## 7. KELVIN AND EDGE WAVES

Long (barotropic) surface waves ($L \gg H$) may be trapped against a straight coast-shelf-slope by the earth's rotation (the Kelvin wave) and by refraction (edge waves) owing to the deeper water and greater local wave speed $(gH)^{1/2}$ offshore. The Kelvin wave propagates cyclonically about the deep sea, has no offshore nodes, and exists at all frequencies $\sigma$ below and above the inertial frequency $f$ according to the longshore wavenumber $k$: $\sigma = \sigma_k(k)$ (HUTHNANCE 1975). Trapping occurs because the Coriolis force piles up the forward-moving water at the wave crest against the coast. Edge waves propagate in either sense with a dispersion relation $\sigma = \sigma_n(k) > |f|$ for the mode with $|n|$ offshore nodes; $n = 1, 2, \ldots$ for cyclonic and $n = 0, -1, -2, \ldots$ for anticyclonic propagation about the deep sea. All edge waves have a low wavenumber cutoff where they cease to be trapped because energy is lost to the deep sea as Poincaré waves (HUTHNANCE, 1975) (perhaps only slowly; LONGUET-HIGGINS, 1967). Particular profiles of depth $h(x)$ for which the Kelvin and edge wave forms have been calculated include a concave exponential $1 - \exp(-ax)$ (BALL, 1967), a uniformly sloping shelf $dx/l$ of width $l$ and maximum depth $d$ meeting the deep sea of uniform depth $D$ at a scarp (MYSAK, 1968) and the step shelf $h = d (0 < x < l)$, $h = D$ $(x > l)$ (MUNK, SNODGRASS and WIMBUSH, 1970).

All continental shelf waves, Kelvin waves and edge waves for a straight shelf and slope of any given depth profile are easily calculated numerically by a method due to LONGUET-HIGGINS (CALDWELL, CUTCHIN and LONGUET-HIGGINS, 1972).

If the shelf is broad and much shallower than the deep sea, then the Kelvin wave is controlled by the major depth change at the shelf edge, rather than by the coast. Well below the inertial frequency, this implies a peak amplitude near the shelf edge (Fig. 6a), i.e. a double Kelvin wave (see section 3; one of the shelf wave modes then usually takes the form of a Kelvin wave against the coast and is essentially confined to the shelf). At the inertial frequency, the Kelvin wave surface elevation for an arbitrary depth profile $h(x)$ is $\exp(ift + iky - kx)$ (Fig. 6a), decaying offshore ($k^2 = f^2/g\bar{h}$ where $\bar{h} \equiv 2k\int_0^\infty h\exp(-2kx)\,dx$ (HUTHNANCE, 1975)). However, the on–offshore flux $hu = if\zeta(0)\exp(kx)\int_0^x (h/\bar{h} - 1)\exp(-2kx)\,dx$ is a maximum near the shelf edge. The longshore current decreases offshore and may reverse in the region of the shelf edge (Fig. 6b). Above the inertial frequency, these same Kelvin wave features typically remain on the broad shelf, except that the offshore elevation decay is not precisely exponential. The on–offshore current maximum near the shelf edge is as large as the longshore shelf currents (Fig. 6b). Approximate scales for an ocean depth $H$, shelf depth $h$ and breadth $L$, and surface elevation $\zeta$ are: deep-sea (offshore, longshore) current $= 0[\sigma L/H,\ (g/H)^{1/2}]\zeta$ respectively; shelf currents $= 0(\zeta)\max[\sigma L/h,\ (g/H)^{1/2}]$ if the shelf is not too broad ($\sigma^2L^2/gh < 1$). Eventually at higher frequencies ($\sigma^2L^2/gh \gtrsim 1$) the shelf is seen as broad and the Kelvin wave becomes trapped against the coast (Fig. 6a).

Kelvin waves are ubiquitous in oceanic surface tides (see next section), and figure prominently in the natural modes of the world's oceans (PLATZMAN, CURTIS, HANSEN and

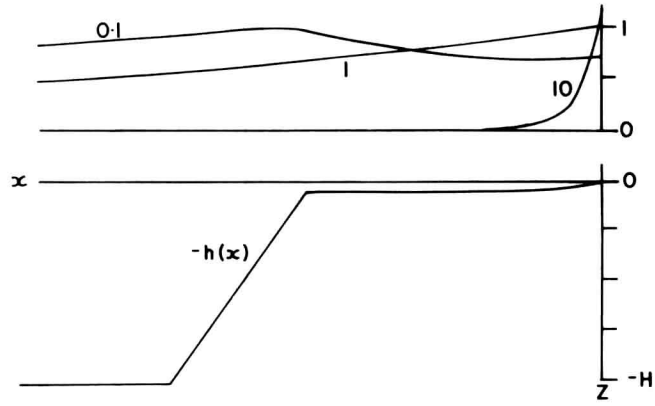


FIG. 6. (a) Kelvin wave elevation profiles for $\sigma/f = 0.1$, 1, 10 where $h = 0.05H\ (1 - \exp(-10 - 5x/L))$ $(-2L < x < 0.5L)$, $h = Hx/L$ $(0.05L < x < L)$, $h = H$ $(x > L)$. $f^2L^2/gH = 0.0156$, $k(gH)^{1/2}/\sigma = 1.294, 1.585, 7.20$ respectively.

SLATER, 1981). Hence in principle they are a natural response to atmospheric pressure forcing. This is most strikingly shown in practice at higher frequencies $\sigma^2L^2/gh \gtrsim 1$, when the wave exists principally over the shallow shelf and naturally responds also to wind-stress forcing, taking over this role from continental shelf waves. Examples are North-Sea storm surges travelling down the east British coast and the response to cyclones along the U.S. east coast (GREENSPAN, 1956), which has been observed to decay from the coast towards the shelf edge (BEARDSLEY *et al.*, 1977).

Edge waves generally have their greatest amplitudes near the coast, particularly when the depth decreases steadily shorewards. The amplitude equation for the surface elevation (HUTHNANCE, 1975) implies an offshore distribution of model structure roughly as $[(\sigma^2 - f^2)/gh + fk(h\sigma)^{-1}\,\mathrm{d}h/\mathrm{d}x - k^2]^{1/2}$, i.e. as $(\sigma^2/gh - k^2)^{1/2}$ at high frequencies: this is clearly weighted towards the coast. Hence edge wave elevations and currents at the shelf edge are expected to be no larger than over the shelf as a whole. Shelf-edge and coastal values may be comparable (Fig. 6c) if the depth is nearly constant across most of the shelf width rather than increasing steadily off-shore. However, edge wave forms decay rapidly seaward of the shelf edge, so that a sharp increase in energy levels shorewards across the shelf edge can be supported. MUNK, SNODGRASS and GILBERT (1964) found that most Southern California shelf energy between tidal frequencies and $10^{-2}$ Hz was contained in such trapped wave modes, rather than exchanging energy with the deep sea.

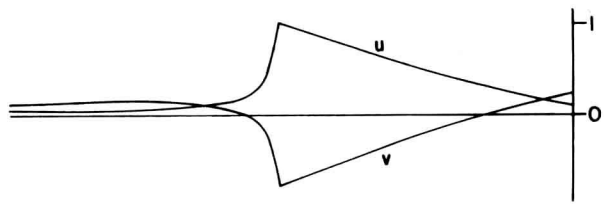


FIG. 6. (b) Kelvin wave onshore ($u$) and longshore ($v$) velocity profiles when $\sigma = f$ in (a). Elevation/velocity scale = 0.0534 $(H/g)^{1/2}$.

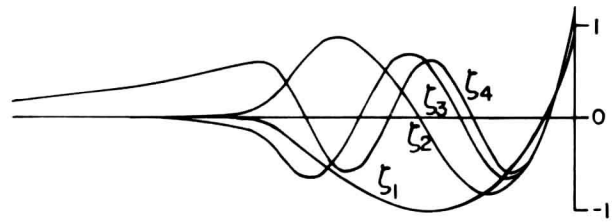


FIG. 6. (c) All edge wave elevation profiles for $\sigma/f = 10$ and the same depth profile. $k(gH)^{1/2}/\sigma = 1.136$, 2.575, 3.753, 4.309 respectively for modes 4, 3, 2, 1.

## 8. BAROTROPIC TIDES

The tides in the oceans and largest adjacent seas are the most common and energetic manifestation of the Kelvin waves discussed above. The shelf width $L$ is usually small enough for $\sigma^2 L^2/gh < 1$ so that the Kelvin waves are basically oceanic with some modification in the region of the shelf. One surprising result is that at latitudes exceeding 30° diurnal tides can be greater at the edge of a broad shelf than at the coast (even without the effects of an additional shelf wave mentioned in Section 3). This appears to be so for the Celtic Sea, where the major O1 and K1 constituents at the shelf edge (CARTWRIGHT, ZETLER and HAMON, 1979) exceed 'coastal' values at Newlyn, St. Mary's and Brest (ADMIRALTY, 1980) although the phases match. Another result from Section 7 is a maximum of on–offshore flux $hu$ at the shelf edge, which is important for internal tide generation (Section 9), and for non-linear generation of harmonics (e.g. M4 from M2) and internal wave trains (Section 10).

Local fits to the tides (usually measured at the coast or on the shelf) by the calculated Kelvin wave form (together with a possible continental shelf wave below the inertial frequency) have been carried out successfully by MUNK *et al.* (1970) for the Californian coast and adjacent ocean and by CARTWRIGHT *et al.* (1980) for the Scottish shelf. The procedure permits extrapolation from the observed tides, particularly across the shelf to the deep sea.

A few areas such as the Argentine shelf and the North Sea are broad and shallow enough for $\sigma^2 L^2/gh \gtrsim 1$, particularly for the semi-diurnal tide. The tide is then dominated by a coastal Kelvin wave (essentially confined to the shelf) with smaller spatial scales and progressing more slowly than the oceanic form.

A major problem in the numerical simulation of ocean or shelf-sea tides is the disparity between oceanic and shelf-sea scales. Oceanic models have difficulty resolving finer shelf length scales, and shelf models including oceanic depths require a drastically reduced time step by the Courant-Friedrichs-Lewy condition $\Delta x/\Delta t > (gh)^{1/2}$ for stable forward integration (e.g. RICHTMYER and MORTON, 1967). The combination of fine scales and oceanic depths requiring short time steps is most formidable at the steep continental slope. A shelf-ocean model of the North-east Atlantic indicates that barotropic tides (but probably only large-scale barotropic motion) can be simulated without detailed resolution of the slope (FLATHER, 1981). However, it is natural (and usual) for oceanic and shelf models to avoid the problem by choosing a shelf-edge model boundary. A boundary condition is then required. In the (usual) absence of detailed knowledge of elevations $\zeta$ or normal fluxes $hu$ at the shelf edge, some specification of a relation between $\zeta$ and $hu$ must be made in an attempt to model the effects of the sea beyond.